ISSN 1063-7710, Acoustical Physics, 2017, Vol. 63, No. 3, pp. 338–345. © Pleiades Publishing, Ltd., 2017.
Original Russian Text © B.M. Salin, O.N. Kemarskaya, P.A. Molchanov, M.B. Salin, 2017, published in Akusticheskii Zhurnal, 2017, Vol. 63, No. 3, pp. 314–322.

OCEAN ACOUSTICS.
HYDROACOUSTICS

# Study of the Mechanism for Broadening of the Spectrum of a Low-Frequency Reverberation Signal for Sound Scattering by Near-Surface Inhomogeneities under Conditions of Intense Wind Waves

**B. M. Salin[a], O. N. Kemarskaya[a], P. A. Molchanov[b], and M. B. Salin[a, *]**

[a] *Institute of Applied Physics, Russian Academy of Sciences, ul. Ul'yanova 46, Nizhny Novgorod, 603950 Russia*

[b] *Kamchatka Hydrophysical Institute, ul. Shvernika 4, Moscow, 117036 Russia*

**e-mail: mikesalin@hydro.appl.sci-nnov.ru*

Received June 6, 2016

**Abstract**—The paper considers the problem of backscattering of sound waves by near-surface volumetric inhomogeneities under conditions of intense wind waves. We calculate the expected share of the scattered signal spectrum based on the given wind-wave intensity and the depth distribution of volumetric inhomogeneities. For deep ocean conditions in the frequency range of 500–1000 Hz for a pulse duration of 10 s, we measure the levels and shape of the reverberation spectrum for time delays from 20 to 100 s. Comparison of the measured and calculated reverberation spectra has shown their good coincidence.

*Keywords*: low-frequency marine reverberation, backscattering, deep ocean, volumetric inhomogeneities, reverberation parameters, calculation of the reverberation spectrum

**DOI:** 10.1134/S1063771017020105

## INTRODUCTION

It is well known that during scattering of low-frequency acoustic waves by surface waves, the spectrum of the reflected signal is broadened. The spectral broadening mechanism is related to two factors. The first is reflection from the fluctuating interface of two media, and the second is scattering by individual subsurface scatterers in motion under the action of wind waves or other factors.

There are quite a lot of experimental studies on evaluating the influence of acoustic wave scattering directly by the sea surface, including monotonic [1, 2] and bistatic [3, 4] scattering of tone pulse and continuous signals. As shown in many works, in particular, [1, 2], for a small Rayleigh parameter, scattering by the spatial wave spectral component $\mathbf{K}$ occurs, which coincides with the difference $\Delta\mathbf{k} = \mathbf{k}_{\text{ind}} - \mathbf{k}_{\text{scatt}}$ of projections onto the horizontal place of wave vectors of an incident $\mathbf{k}_{\text{ind}}$ and scattered $\mathbf{k}_{\text{scatt}}$ acoustic wave. For the indicated model in the case of Bragg backscattering, the reverberation spectrum should contain two spectral components at frequencies $F_0 \pm \sqrt{2kg}/2\pi$. Here $F_0$ is the ranging signal (Hz), $k$ is the wave vector of the acoustic wave, and $g = 9.8$ m/s$^2$ is freefall acceleration.

As numerical calculations have shown [5], for a large value of the Rayleigh parameter, qualitatively, the pattern of the reverberation spectrum does not change, but the spectral peaks at frequencies $F_0 \pm \sqrt{2kg}/2\pi$ become significantly wider with an increase in the Rayleigh parameter.

The experimental data, in particular, presented in [1, 2], demonstrate that the real backscattering spectrum is bell-shaped with the center at the carrier frequency $F_0$ and with significantly smaller peaks in the frequency domain $F_0 \pm \sqrt{2kg}/2\pi$.

To substantiate and simulate the experimentally observed bell shape of the low-frequency monostatic reverberation spectrum at frequency $F_0$, we will use the model of sound wave reflection from moving volumetric subsurface scatterers, which may be, e.g., a sheet of bubbles that occurs during the breaking of intense wind waves [6]. The characteristic depth to which waves propagate is $z \sim \Lambda = 2\pi/K_m$, where $K_m$ is the minimum value of the wave vector of wind waves in the water area. For a wind wave frequency of ~0.1 Hz, the characteristic depth $z$ of penetration of oscillations is a significant value, ~100 m.

## MODEL OF THE SPECTRA OF A SIGNAL SCATTERED BY SUBSURFACE INHOMOGENEITIES

To describe the characteristics of developed surface waves, we chose the most widespread Pierson–Moskowitz model spectrum, which gives the spectral power density of waves in the form

$$G^2(\Omega) = 0.0083\frac{g^2}{\Omega^5}e^{-0.74\left(\frac{g}{\Omega V}\right)^4}, \text{ or}$$
$$G^2(\Omega) = 0.0083\frac{g^2}{\Omega^5}e^{-1.25\left(\frac{\Omega_m}{\Omega}\right)^4}, \quad (1)$$

where $V$ is the wind speed(m/s) at the 10–20 m horizon and $\Omega_m$ is the frequency of the maximum of the wave spectrum.

Integrating expression (1) over $\Omega$, we can obtain the mean square value of the amplitude of surface oscillations (wave amplitude) $\sigma = \sqrt{\overline{(x-\bar{x})^2}}$ for a fixed value of the wind speed or frequency of the maximum of the wave spectrum.

We will consider surface oscillations at a local point with a relatively narrowband process. Estimates show that for a wind speed of, e.g., $V = 13$ m/s (~50 km/h), which corresponds to $\Omega_m = 2\pi \times 0.1$ Hz,the mean square value $\sigma$ of the wave amplitude in nearly the entire frequency band from 0 to 1 Hz is 1 m and the analogous value in the band $\delta f = 0.05$ Hz in the vicinity of the maximum of the wave spectrum $f_m = \Omega_m/2\pi = 0.1$ Hz is $\sigma_{0.1\text{Hz}} = 0.78$ m or 60% of the total wave energy.

The choice of a relatively narrow wave spectrum band ($\delta f/f_m = 0.5$) makes it possible to simplify calculation of the scattered tone pulse signal. To find the field of the current in the near-surface layer, we will use the model of a sinusoidal surface wave, whose wavenumber $K_m$ corresponds to the maximum of the wave spectrum, and the amplitude is determined by the mean square value of the wave amplitude in the mentioned frequency band.

In the linear case in the absence of stationary currents and the influence of the bottom, the motion trajectory of a fluid element in the vicinity of a point with depth $z$ is a circle the radius $R(z)$ of which (see Fig. 1) has an exponential dependence on the deepening of $z$:

$$R(z) = R_0\exp(-K_m z), \quad (2)$$

where $R_0$ is the averaged value of the wave amplitude on the surface in the frequency band from $0.75f_m$ to $1.25f_m$.

Let us find the Doppler spectrum of a signal scattered by a fluid element of volume $\Delta U$, which is located at a mean depth $z$ and is moving in the vertical plane along the circumference of radius $R(z)$ with a cyclical frequency $\Omega_m$. Let us assume that the projection of its linear velocity in the direction of propagation of the acoustic wave varies in the range $\pm R(z)\Omega_m$ according to the law

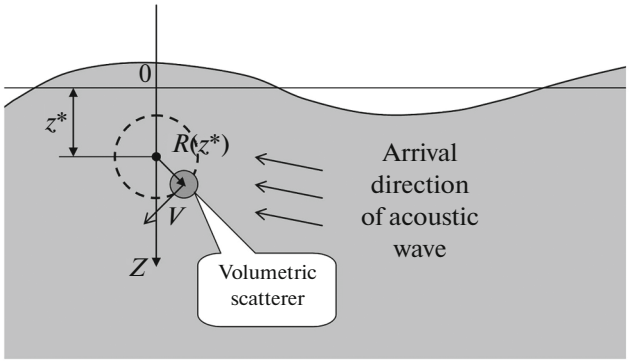


**Fig. 1.** Scheme for calculating sound scattering by subsurface scatterers.

$$u_x = R(z)\Omega_m \sin(\Omega_m t).$$

Let us consider the problem of determining the spectrum of the signal, which is scattered by a rotating irregularity with an isotropic angular radiation pattern. This problem is not going to be solved via the Fourier transform of the signal, followed by incoherent accumulation of spectra, but in a simpler way. Let the scattered signal from the receiver be preliminarily passed to a heterodyne and then be passed in complex form to a set of $2N$ bandpass filters, when the passband of the $n$th filter is $n\Delta f$ to $(n+1)\Delta f$, including both positive and negative ($n < 0$) Doppler frequencies.

If the Doppler frequency of the backscattered signal varies according to the sine function $f_{\text{dop}}(t) = 2u_x/\lambda = (2R(z)\Omega_m/\lambda)\sin(\Omega_m t)$, then the equation $n\Delta f = (2R(z)\Omega_m/\lambda)\sin(\Omega_m t_n)$ helps to find the time when the frequency $f_{\text{dop}}(t)$ crosses the passband of the $n$th filter. This happens once per semiperiod $T/2 = \pi/\Omega_m$. Next, we can use values of $t_n$ and $t_{n+1}$ to determine the time interval when the Doppler frequency stays inside the passband of the $n$th filter:

$$\Delta t_n = t_{n+1} - t_n$$
$$= \frac{1}{\Omega_m}\text{Re}\left(\arcsin\frac{\lambda(n+1)\Delta f}{2\Omega_m R(z)} - \arcsin\frac{\lambda n\Delta f}{2\Omega_m R(z)}\right). \quad (3)$$

The following property is used here: $\text{Re}(\arcsin\xi) = \pi/2$ for $\xi \geq 1$ and $\text{Re}(\arcsin\xi) = -\pi/2$ for $\xi \leq -1$.

We can easily find that the final distribution of the scattered signal intensity over the frequency channel numbers is proportional to the found durations of stay of the signal in the frequency channels, with the

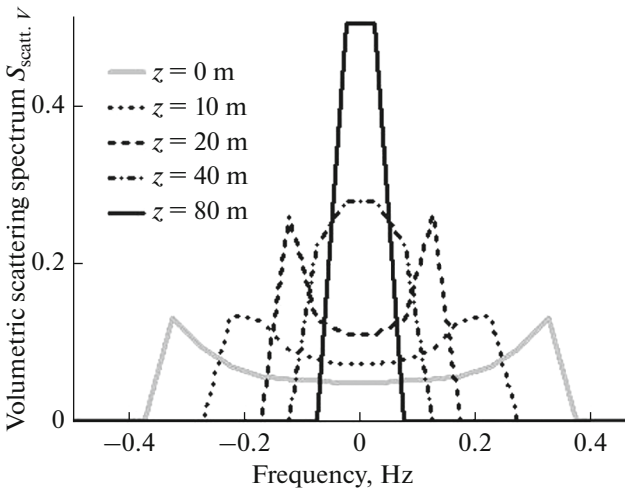


**Fig. 2.** Spectrum of volumetric scattering strength $S_{\text{scatt.}V}(z, f)$, constructed for different depths $z$ of scatterer location, in decibel scale.

respect to the normalization by the total observation time T/2.

$$\Delta P^2(\rho, z, n) = \frac{\Delta P^2(\rho,z)}{\pi} \times \mathrm{Re}\left(\arcsin\frac{\lambda(n+1)\Delta f}{2\Omega_m R(z)} - \arcsin\frac{\lambda n\Delta f}{2\Omega_m R(z)}\right). \quad (4)$$

Here, $\Delta P^2(\rho, z, n)$ is a squared amplitude of the signal, scattered by $\Delta U$ and filtered in the band from $n\Delta f$ to $(n + 1)\Delta f$. $\Delta P^2(\rho, z, n)/\Delta f$ is a power spectral density of the received signal. $\Delta P^2(\rho, z) = \left(S_{\text{scatt.}V}(z)\Delta U\right) P_{\text{lm}}^2\, \mathrm{TL}^4(\rho)$ is a total squared amplitude of the signal, scattered by $\Delta U$ element. $S_{\text{scatt. }V}(z)$ is the strength of volumetric sound scattering in a medium in the inverse direction ($1/\text{m}^3$), $\Delta U = \Delta z\ \Delta\rho\ \Delta\varphi\ \rho$ is the volume of the elementary scatterer, $\rho$ is the distance from the scatterer to the receiver–emitter, TL is propagation losses (taken in a linear scale), and $P_{\text{lm}}^2$ is the field at a distance of 1 m from the source ($\text{Pa}^2$).

Obviously, the sum of the squares for all frequencies of the spectrum is equal to the initial power of the signal scattered by $\Delta U$, $\Delta P^2(\rho,z) = \sum_{n=-N}^{N} \Delta P^2(\rho, z, n)$.

The following expression for $\Delta P^2(\rho, z)$ as a function of the parameters of the scatterers can be substituted to (4)

$$\Delta P^2(\rho, z, n) = P_{\text{lm}}^2 \mathrm{TL}^4(\rho) \times \left\{\frac{1}{\pi}\mathrm{Re}\left(\arcsin\frac{\lambda(n+1)\Delta f}{2\Omega_m R(z)} - \arcsin\frac{\lambda n\Delta f}{2\Omega_m R(z)}\right) S_{\text{scatt.}V}(z\right\}\Delta U, \quad (5)$$

and by analogy with (3) one can introduce and calculate the spectral characteristic of the volumetric scattering strength:

$$S_{\text{scatt.}V}(z, n) = \frac{1}{\pi}\mathrm{Re}\left(\arcsin\frac{\lambda(n+1)\Delta f}{2\Omega_m R(z)} - \arcsin\frac{\lambda n\Delta f}{2\Omega_m R(z)}\right) S_{\text{scatt.}V}(z). \quad (6)$$

Figure 2 shows for example the result of calculating the dependences of the level of the volumetric scattering strength spectrum $S_{\text{scatt.}V}(z, f)$ for a volumetric element at depths $z$ 0, 20, and 80 m, for a single value of the volumetric scattering strength ($S_{\text{scatt.}V}(z) = 1/\text{m}^3$). Calculation was performed for the following parameters mentioned above: $\lambda = 3$ m ($F_0 = 500$ Hz), $\Delta f = 0.1$ Hz, $n = -25$ to $+25$, frequency of the energy-carrying wave component $\Omega_m = 2\pi \times 0.1$ Hz (which corresponds to a wind speed of $V = 13$m/s or 25 knots).

As one can see from the figure, the width of the scattered signal spectrum varied from 0.8 Hz for a small scatterer depth to a spectral analysis resolution of ~0.1 Hz at scatterer depths of 80 m or more.

When integrating (6) over $z$ taking into account expression (2), we pass from the spectral characteristic of the volumetric scattering strength $S_{\text{scatt. }V}(n)$ to scattering by the entire vertical fluid column $n$–the spectral characteristic of the surface scattering strength $S_{\text{scatt.}S}(n)$, where $n$ is the number of frequency channels $f_n = (n + 0.5)\Delta f$:

$$S_{\text{scatt.}S}(n) = \frac{1}{\pi}\int_0^\infty \mathrm{Re}\left(\arcsin\frac{\lambda(n+1)\Delta f}{2\Omega_m R(z)} - \arcsin\frac{\lambda n\Delta f}{2\Omega_m R(z)}\right) S_{\text{scatt.}V}(z)dz. \quad (7)$$

In expression (7), there is an unknown function $S_{\text{scatt.}V}(z)$, the dependence of the volumetric scattering strength on depth. We use two independent approaches to estimate this value.

In the first, in analogy to (2), we represent the volumetric scattering strength as the exponential dependence on depth plus a constant:

$$S_{\text{scatt.}V}(z) = S_{\text{scatt.}V} + S_{\text{scatt.}V}^{\text{wind}} \exp(-z/z_0), \quad (8)$$

where the constant $S_{\text{scatt.}V}$ is the classical value of the volumetric scattering strength in the range of 0.5–1, equal to −100 to −80 dB [7]; $S_{\text{scatt.}V}^{\text{wind}}$ is the value of the volumetric backscattering strength close to the free surface; $z_0$ is the characteristic distance when the volumetric scattering determined by the amount of bubbles and other dislocations decreases with distance from the surface $e$ times.

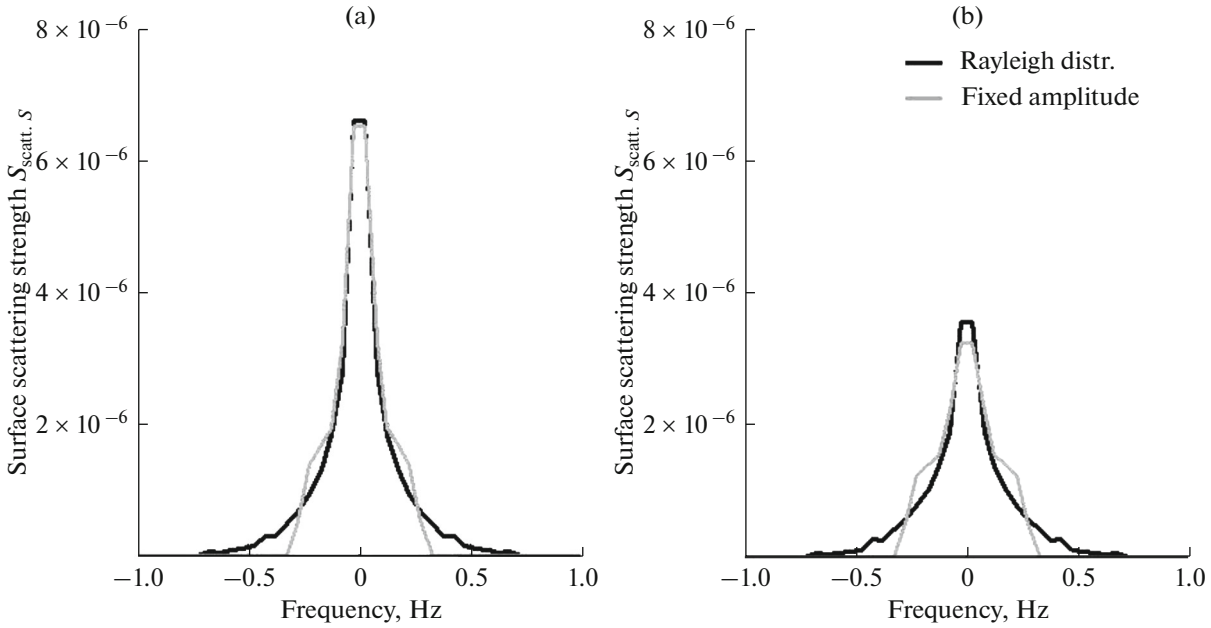


**Fig. 3.** Spectrum of surface scattering strength $S_{\text{scatt.}S}(f)$, constructed in decibel scale: for two values of depths $z_0$, 30 and 20 m ((a) and (b), respectively), for a fixed value of wind wave amplitude 0.74 m (light curve) and wind waves, the amplitudes of which are distributed according to the Rayleigh law (dark curve).

Figures 3a and 3b show the backscattering spectra $S_{\text{scatt.}S}(f)$ calculated for values of $S_{\text{scatt.}V} = 10^{-9}$ 1/m$^3$, $S^{\text{wind}}_{\text{scatt.}V} = 10^{-6}$ 1/m$^3$ and two characteristic depths of the decrease in the volumetric scatterers $z_0 = 20$ and $z_0 = 30$ m (light curves in Fig. 3). The $S^{\text{wind}}_{\text{scatt.}V}$ and $z_0$ values were chosen such that (a) the volumetric scattering strength $S_{\text{scatt.}V}(z)$ does not depend a priori on $z$ for depths greater than 200 m and (b) the calculated shape of the reverberation signal spectrum coincides with the experimental data to the maximum extent.

Based on the adopted value of the volumetric scattering strength $S_{\text{scatt.}V} = 10^{-9}$ 1/m$^3$ without allowance for the $S^{\text{wind}}_{\text{scatt.}V}$ value, we can estimate the contribution of volumetric scattering to the exponential sound attenuation. As calculations have shown, the contribution to attenuation is a negligible value of 0.054 dB per 1000 km.

When calculating the plots in Fig. 3, in (7) we integrated to a depth of 1000 m. The contribution of scattering independent of the $z$ component $S_{\text{scatt.}V}$ to the spectrum was ~+10% at frequency $F_0$.

When calculating the surface scattering spectrum in form (8), we did not take into account a random direction of wave movement (this will lead on average to narrowing of the spectra in Fig. 3 by approximately 30%) and the random character of the wind wave height. If we take into account that the wave amplitude $R_0$ is distributed according to the Rayleigh law, then we can recalculate the scattering spectra by introducing into (7) a Rayleigh distribution that depends on the variable $R_0$ and the mean wave value $\overline{R_0}$:

$$\overline{S_{\text{scatt.}S}(n)} = \frac{1}{\pi}\int_0^\infty \frac{R_0}{\left(\overline{R_0}\right)^2}\exp\left(\frac{-R_0^2}{2\left(\overline{R_0}\right)^2}\right) \times \int_0^\infty \operatorname{Re}\left(\arcsin\frac{\lambda(n+1)\Delta f}{2\Omega_m R(z)} - \arcsin\frac{\lambda n\Delta f}{2\Omega_m R(z)}\right) \times S_{\text{scatt.}V}(z)dz\,dR_0. \quad (9)$$

Figure 3 also shows plots of the averaged surface scattering spectra calculated according to (9) for $\overline{R_0} = 0.74$ m, a wind speed $V = 13.7$ m/s, and two values $z_0 = 20$ and $z_0 = 30$ m (dark curves).

Summing the surface scattering strength over all frequencies,

$$S_{\text{scatt.}S} = \sum_n S_{\text{scatt.}S}(n), \quad (10)$$

we obtain the lower boundary of the conventional value of the scattering strength on the surface for around a zero grazing angle and a given wave or wind strength amplitude value[1].

[1] For a small grazing angle, sound scattering directly by the surface of the water area will be minimal and scattering by subsurface inhomogeneities will remain virtually unchanged and in fact will determine the boundary value of the total scattering strength.

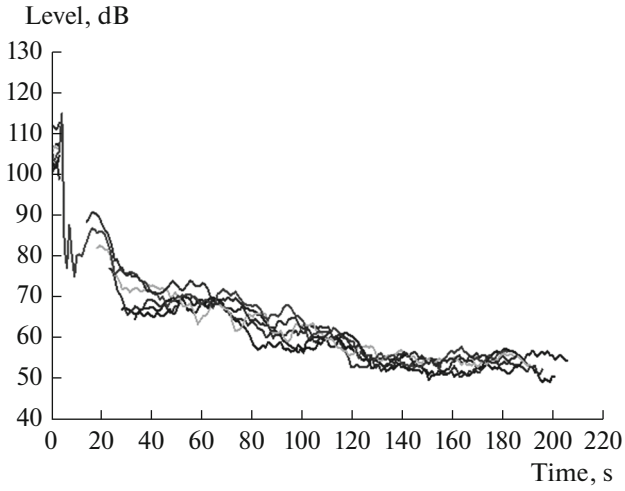


**Fig. 4.** Dependence of reverberation level on time for frequency grid in range of 700–800 Hz. Direction −75° from normal of receiver array.

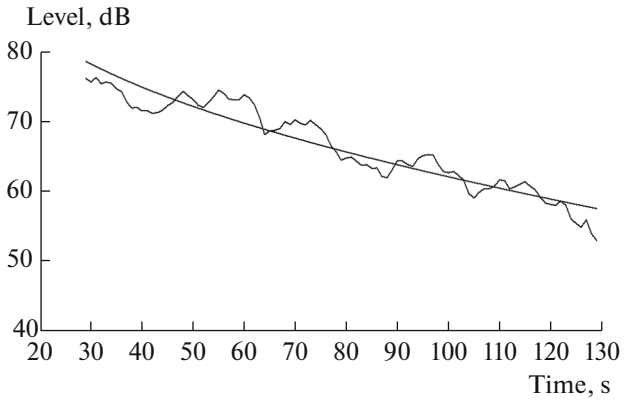


**Fig. 5.** Dependence of reverberation level of time for frequency grid in range of 700–800 Hz. Direction of −75° from normal of receiver array. Time dependence of reverberation level: experimental curve and approximating curve (smooth) $I_r(t) = I_{r_0}(ct)^{-2} \times 10^{-0.1\beta ct}$ ($\beta = 0.054$; $I_{r_0} = 2 \times 10^{11}$), decibel scale, frequency $F_0 = 800$ Hz.

As calculations have shown, the $S_{\text{scatt.}S}$ values attained according to (7) and (9) for a wind strength of 25 knots are −47 dB ($z_0 = 20$ m) and −45 dB ($z_0 = 30$ m), which agrees with the experimental data of [8] obtained for small grazing angles at frequencies of 0.5–1 kHz for a wind speed of 25 knots. Such a comparison is possible, because the intensity of the signal scattered directly by an uneven water–air boundary decreases with a decreasing grazing angle.

Based on the obtained value of background scattering with a 1 m$^2$ surface, we can easily pass to integral estimation of the target strength of background scattering for the monostatic ranging scheme $\text{TF}_{\text{back}} = S_{\text{scatt.}S}\frac{cT}{2}\Delta\varphi\frac{ct}{2}$. For example, for a pulse duration of $T = 10$ s, a time delay of $t = 40$ s (a distance of ~30 km) and angular resolution of the receiver array of $\Delta\varphi = 0.1$ rad, the level of the background target strength at frequency $F_0$ is $\text{TF}_{\text{back}} = 26$ dB.

Indirect verification of the coincidence of the experimental and calculated values shows that for a wind speed of 25 knots, the numerical values entering into Eq. (8) werecorrectlychosen.

The second method of estimating $S_{\text{scatt.}V}(z)$ relies on experimental measurement of the depth and radius distributions of the bubble concentrations, which is presented in [9] with reference to [10]. All existing bubble fractions have resonance frequencies significantly higher than the considered frequency $F_0 = 500$ Hz, and the scattering strength can be calculated by well-known method [9]. Unfortunately, the presented data have a selective character: for a wind speed of 11–13 m/s and three horizons. The result of calculating the scattering strength only for the given bubble distribution without allowance for other scatterers can be expressed using the notation introduced above: $z_0 = 1.6$ m, $S^{\text{wind}}_{\text{scatt.}V} = 1.9 \times 10^{-7}$ 1/m$^3$. The estimates show that the resulting value for the strength of scattering by bubbles at a frequency of 500 Hz is a small value: $S_{\text{scatt.}S.\text{bubbl.}} = -66$ dB.

In [6], it was noted that air cavities and bubble clouds can form, the gas concentration in which is by two to four orders of magnitude higher than in the background bubbles. Thus, the estimate $S_{\text{scatt.}S} = -45$ to −47 dB used above can be considered quite realistic and valid. The existing uncertainty in the input data on the concentration and dimensions of air formations does not allow more exact calculations and removes the necessity of taking into account fine diffraction effects during sound scattering by bubbles, as was done, e.g., in [6].

## RESULTS

In 2011, we studied the characteristics of reverberation signals in oceanic conditions: the Pacific Ocean, the region of the Kamchatka Peninsula. These studies were a continuation of experimental works conducted in this region since the mid-1980s. A partial description of the results of earlier studies is given in [11, 12], which studied the energy characteristics of reverberations in the frequency range of 600 and 800 Hz with tone pulse signals with a duration of ~5–10 s used for ranging.

As studies [12] have shown, the time dependence of the reverberation level in these conditions is well described by the expression

$$I_r(t) = I_{r0}(ct)^{-n} \times 10^{-0.1\beta ct}, \qquad (11)$$

where $c = 1.47$ km/s, $n = 2$, and $\beta \approx 0.03$–$0.08$ dB/km. The value $n = 2$ corresponds to a decrease in sound intensity with distance according to the law $r^{-3/2}$, and the experimentally obtained $\beta$ values somewhat exceed the theoretical dependence $\beta = 0.036f^{3/2}$ dB/km ($f$ is in kilohertz). The theoretical $\beta$ value for $f = 0.6$ kHz is 0.017 dB/km.

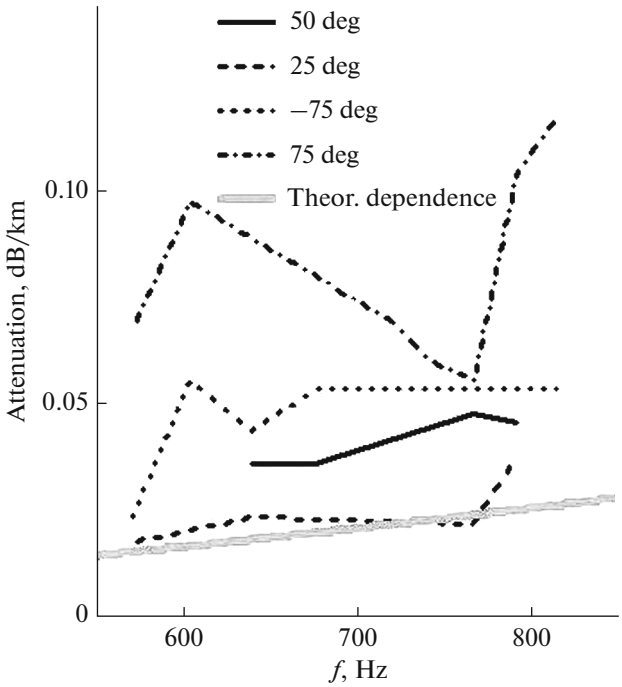


**Fig. 6.** Experimentally measured dependences $\beta(F_0)$ for four directions of signal reception. Gray curve, theoretical dependence $\beta = 0.036\ (10^{-3}f)^{3/2}$ dB/km ($f$ in hertz).

Based on our data obtained in 2011, in analogy with [12], we also constructed the dependences of the reverberation level for certain frequencies and directions of signal reception, which was performed with a directional receiver array. Thus, e.g., Fig. 4, for a pulse duration of 10 s and a direction of −75% from the normal of the array, shows the dependences of the reverberation level on time in a band of 1 Hz for an arbitrary set of frequencies taken in the range of 700–800 Hz. Here and below, 0 dB is taken as the uncertain level. As one can see from the figure, the frequency scatter of the emission level and reverberation level did not exceed 10 dB.

To determine parameter βwe approximated the adopted reverberation signal by a function of the form (11) $P^2_{\text{approx}}(t) = I_{R_0}(ct)^{-2} \times 10^{-0.1\beta ct}$ where $c = 1.45$ cm/s and β is in dB/km. Unknown parameters $I_{R_0}$ and β were found in the time interval of 30–130 s from the minimum of the difference in the reverberation levels $(\min\left|10\log P^2_{\text{exp}}(t) - 10\log P^2_{\text{approx}}(t)\right|)$, expressed in a decibel scale.

Figure 5 shows, e.g., in the decibel scale, the approximated dependence and reverberation curve measured for a direction of −75°. Figure 6 shows the data on the frequency dependences β obtained for four directions of signal reception. Nearly all the β values turned out to be larger than the theoretical ones shown in Fig. 6 by the gray curve. The scatter of the measured βvalues for difference directions is mostly likely the result of the significant difference of the bottom profile and the hydrology along the indicated propagation tracks for the direct and scattered signals. Some of the directions correspond to deep ocean conditions and some are closer to shelf zone conditions.

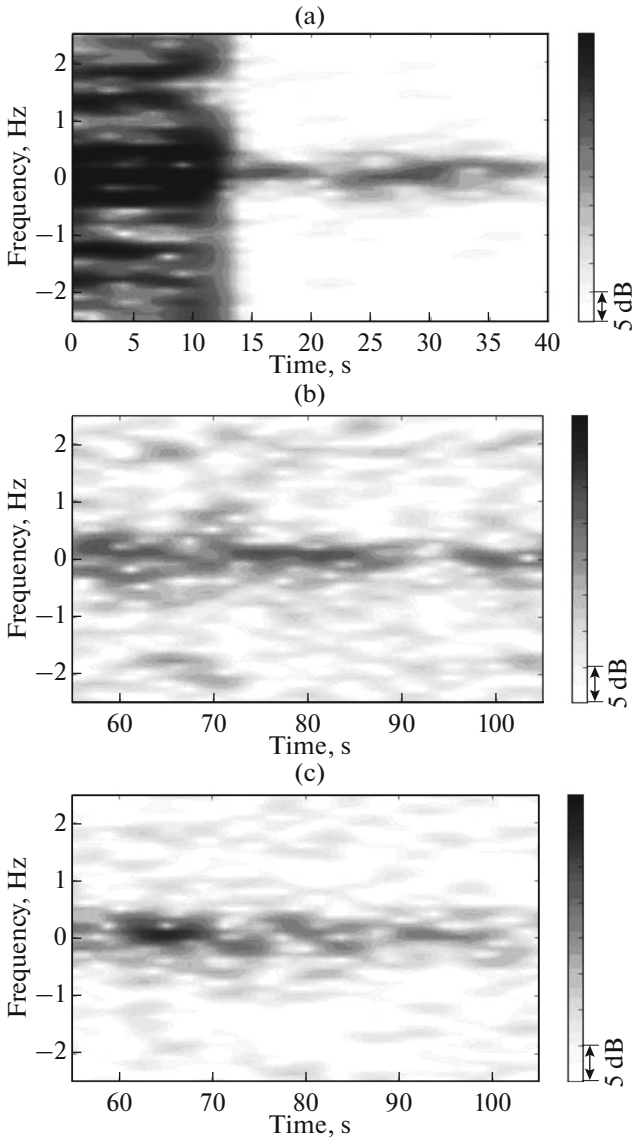


**Fig. 7.** Current spectra of heterodyne reverberation signals measured for emission frequencies of $F_0 \approx 600$, 700, and 800 Hz (Figs. 7a–7c, respectively).

To study the reverberation spectra we performed current spectral analysis of a reverberation signal with the maximum frequency resolution of $\Delta f = 0.1$ Hz, which was determined by the duration of the ranging pulse. For example, Fig. 7 shows in a decibel scale the current spectra of heterodyned reverberation signals for emission frequencies $F_0$, near frequencies of 600, 700, and 800 Hz. The time in the spectra is counted with respect to the instant a pulse reached the receiver system. Figure 7a shows a fragment of a spectrogram that includes the instant of arrival of a direct signal.

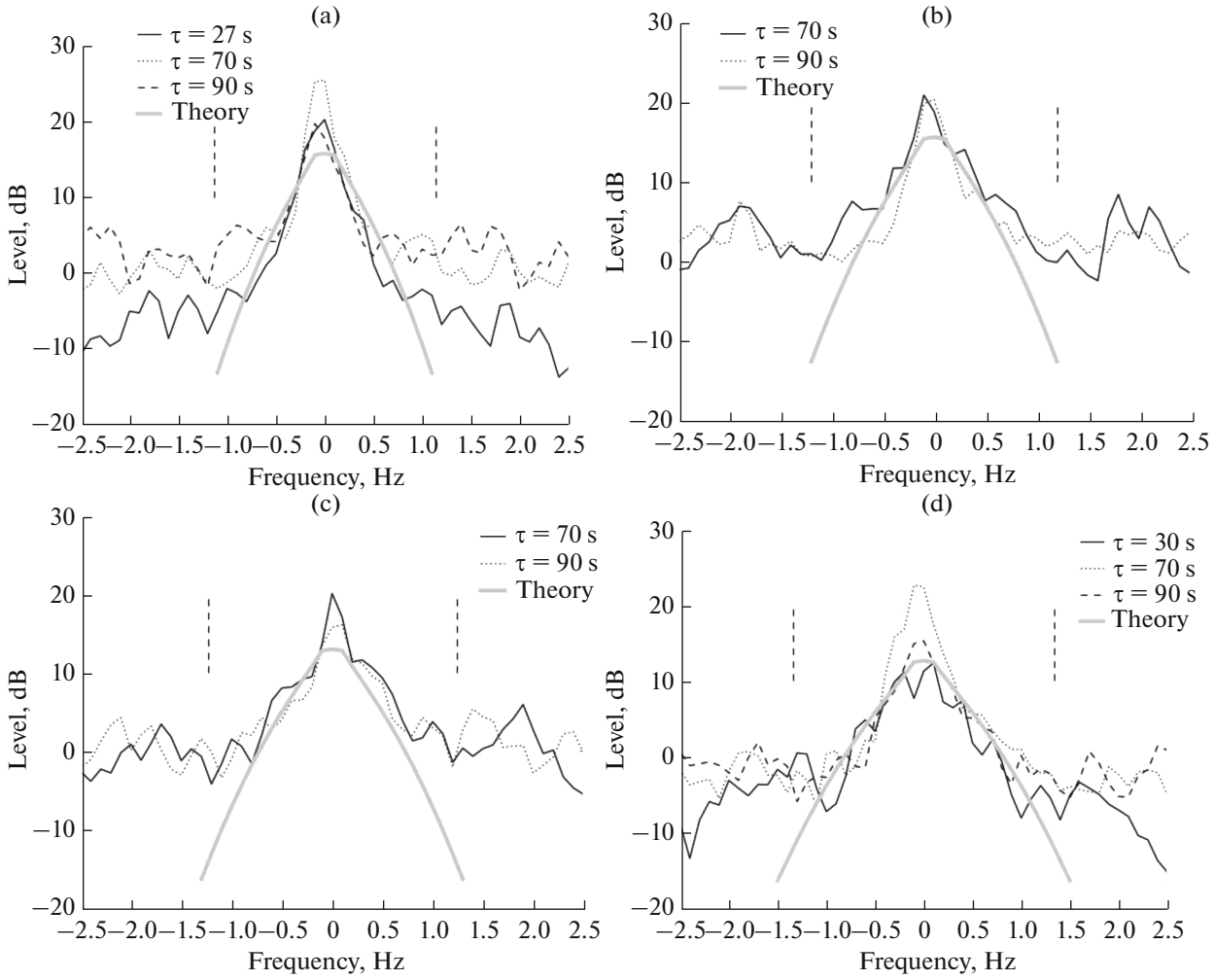


**Fig. 8.** Averaged and orthonormalized reverberation spectra $\tilde{S}_m(F_0, f)$, constructed for tone pulse signals in the frequency range 500–800 Hz, in order of increasing frequency passing from Fig. 8a to Fig. 8b. Wide gray line corresponds to theoretical shape of spectrum calculated according to (9).

The direct signal is depicted with a color-scale limitation and, in addition, due to the operational features of the recording system, a rise in the background level is observed in the entire frequency range at the instant of signal arrival.

As one can see from the spectrograms, reverberation at the carrier frequency exceeds the background values of the spectrum in the entire measurement time. The width of the reverberation spectrum is ~1 Hz. As well, the driving generator of the emitter is sufficiently stable, and the width of the spectrum of the direct signal is determined only by the duration of the pulse envelope, which is 5–10 s.

To study the shape of the reverberation signal at different arrival times and compare it to the theoretical dependence, we averaged the current spectra in a time interval of ~20 s for the time instants $\tau_m$ = 30, 70, and 90 s. Based on the experimental dependence of the reverberation level on time delay $\tau$ in form (11) $I_r(\tau) \sim I_{r0}(c\tau)^{-2}$, we normalized the averaged reverberation spectra $S_m(F_0, f)$ to a value of

$$\tilde{S}_m(F_0, f) = S_m(F_0, f)\left(\frac{\tau_m}{\tau_*}\right)^2 A(F_0), \qquad (12)$$

where $\tau_*$ is the mean time in the measurement interval ($\tau_*$ = 50 s). The normalizing factor $A(F_0)$ was chosen such that the reverberation level at the zero frequency $\tilde{S}_m(F_0, 0)$ was the conditional value ~20 dB for all $F_0$, independently of the emission level.

Figure 8 shows the averaged and orthonormalized reverberation spectra $\tilde{S}_m(F_0, f)$ constructed for the frequency range $F_0$ 500–800 Hz and time delays = 30, 70, and 90 s. The excess of the averaged reverberation spectrum level at frequency $f$ = 0 over the background value was 15–30 dB, depending on the value of the time delay.

According to meteorological archive data [13], the wind speed during the experiments in the given region was 15–20 knots. Estimates of the scattering spectrum were obtained for a wind speed close to the mentioned values; therefore, they can be compared to the experimental data.

The theoretical dependence in Fig. 8 (wide gray line) was constructed according to (9) for the above-mentioned wave and scattering parameters of the form $S_{\text{scatt.}V} = 10^{-9} + 10^{-6} \times \exp(-z/20)$. As one can see from comparison of the plots, at nearly all carrier frequencies $F_0$ and delay times from 30 to 100 s, the measured reverberation spectra correspond well to the calculated ones in width and shape, as well as in the steepness of the drop with difference frequency $f$.

## CONCLUSIONS

In closing it should be noted that the presented schemes make it possible to calculate the spectral characteristics of reverberation for the monostatic ranging scheme and the use of low-frequency tone pulse signals. Calculations are performed based on certain data on the propagation conditions, knowledge of the wind wave amplitude, and the depth distribution of the local volumetric scattering strength. If the mentioned data are available, the proposed calculation scheme can be used to predictively estimate the shape and width of the reverberation spectrum. In setting up special experiments with measurement of the reverberation parameters, propagation conditions, and wind wave level, it is possible to solve the inverse problem: reconstruction of the depth distribution of the strength of volumetric scatters.

## ACKNOWLEDGMENTS

B.M. Salin and M.B. Salin thank the Russian Science Foundation (RSF, grant no. 14_17_00667) for support of theoretical research. Development of signal processing methods was partially supported by the RSF program of states' academies of sciences for 2013–2020, section no.12.18 "Development of Physical Foundations of New-Generation Acoustic Systems." Experimental research was conducted by the Kamchatka Hydrophysical Institute.

## REFERENCES

1. B. C. Averbakh, L. F. Bondar', V. N. Golubev, V. Yu. Gol'dblat, L. S. Dolin, A. G. Nechaev, K. E. Pigalov, G. E. Smirnov, and E. I. Tumaeva, Akust. Zh. **36** (6), 1119–1121 (1990).
2. D. I. Abrosimov, V. S. Averbakh, E. I. Bolonicheva, V. N. Golubev, V. Yu. Gol'dblat, L. S. Dolin, A. G. Nechaev, K. E. Pigalov, and N. I. Sirotkina, Akust. Zh. **41** (3), 364–369 (1995).
3. I. B. Andreeva and V. N. Lupovskii, Akust. Zh. **39** (4), 565–574 (1993).
4. B. M. Salin and M. B. Salin, Acoust. Phys. **57** (6), 833–842 (2011).
5. M. B. Salin, A. S. Dosaev, A. I. Kon'kov, and B. M. Salin, Acoust. Phys. **60** (4), 442–454 (2014).
6. T. H. Neighbors and L. Bjerne, Hydroacoustics **4**, 181–192 (2001).
7. I. B. Andreeva, Akust. Zh. **41** (5), 699–705 (1995).
8. R. J. Urick, *Principles of Underwater Sound*, (McGraw-Hill, New Yotk, 1975)
9. L. M. Brekhovskikh and Yu. P. Lysanov, *Theoretical Foundations of the Ocean Acoustics* (Springer-Verlag, New York, 2003).
10. P. A. Kolobaev, Okeanologiya **15** (2), 1013–1017 (1975).
11. R. A. Vadov, D. V. Guzhavina, and S. I. Dvornikov, Acoust. Phys. **43** (3), 350–352 (1997).
12. D. V. Guzhavina and E. P. Gulin, Acoust. Phys. **47** (4), 398–404 (2001).
13. *The Advanced Scatterometer (ASCAT) Data Products.* Center for Satellite Application and Research. NESDIS. url: manati.star.nesdis.noaa.gov/datasets/ ASCAT-Data.php/ASCATData.php

*Translated by A. Carpenter*